Chemical Science

ROYAL SOCIETY OF CHEMISTRY

EDGE ARTICLE

View Article Online
View Journal | View Issue

Cite this: *Chem. Sci.*, 2025, **16**, 20495

All publication charges for this article have been paid for by the Royal Society of Chemistry

Received 17th April 2025
Accepted 30th September 2025

DOI: 10.1039/d5sc02831k

rsc.li/chemical-science

Enantioselective homocoupling of allenylic alcohols through divergent cooperative catalysis

Aditya Chakrabarty, Ritwika Chatterjee and Santanu Mukherjee *

An enantioselective homocoupling of branched allenylic alcohols is developed under cooperative iridium and Lewis acid catalysis. In this reaction, racemic allenylic alcohol is transformed, under Lewis acidic $Sc(OTf)_3$, into an α,β-unsaturated enol (cross dienol) through a Meyer–Schuster-type 1,3-hydroxy transposition. In an independent cycle, catalyzed by a combination of an Ir(I)/(phosphoramidite,olefin) complex and $Sc(OTf)_3$, allenylic alcohol is proposed to produce an η^2-Ir(I)-bound allenylic carbocation intermediate, which is intercepted by the *in situ* generated cross dienol. Overall, starting from racemic branched allenylic alcohols, α′-allenylic α,β-unsaturated ketones are produced, without using any preformed carbon nucleophile, in moderate to good yields with excellent enantioselectivities. This strategy may be termed as *divergent cooperative catalysis*, where a single substrate is converted into two transient intermediates of complementary polarity under the influence of two different catalysts. The selective coupling of these two polarity-matched intermediates results in the desired product. Mechanistic details are unraveled through experimental studies and density functional theory (DFT) calculations.

Introduction

Cross-coupling reactions represent a highly effective approach for constructing carbon–carbon (C–C) and carbon–heteroatom (C–X) bonds, which typically require two reaction partners. In contrast, coupling reactions involving a single substrate can be envisioned, where the substrate would be converted into two transient intermediates of complementary polarity under the influence of two different catalysts (Fig. 1A). Selective merging of these two polarity-matched intermediates would lead to the desired homocoupling product. This type of homocoupling reaction is rare and conceptually different from classical homocoupling processes such as self-aldol or benzoin condensation, where a catalytically generated reactive nucleophile couples with the unmodified electrophilic substrate. This hitherto unprecedented catalytic strategy can be termed as *divergent cooperative catalysis* and is fundamentally different from the traditional cooperative catalysis (Fig. 1B),[1] which begins with two substrates of complementary polarity. Usually, the role of catalysts in the latter case is to enhance the innate reactivity of each substrate.

The prerequisite of divergent cooperative catalysis is the identification of an ambiphilic substrate[2] which is amenable to different activation mechanisms towards intermediates of complementary polarity under different types of catalysis. More specifically, substrates traditionally recognized as electrophiles need to be converted into nucleophiles or *vice versa*. Such processes (*e.g.*, cross-electrophilic coupling) usually involve redox manipulation of either the substrate or the catalyst.[3] However, catalytic homocoupling reactions under redox-neutral conditions is highly desirable as it would comply with the economy of synthesis.[4]

The implementation of the concept of divergent cooperative catalysis with substrate identification, catalyst optimization and mechanistic elucidation is presented herein.[5]

Allenylic alcohols and their derivatives are generally employed as electrophiles in transition metal-catalyzed substitution reactions (Scheme 1A).[6–8] In this context, the Ir(I)/(phosphoramidite,olefin) catalyst system introduced by Carreira *et al.*, is particularly noteworthy.[7] With racemic branched allenylic alcohol as the substrate, this Ir(I)-complex in combination with a Lewis acidic promoter is proposed to generate an η^2-Ir(I)-bound allenylic carbocation intermediate (**A**), which generally exhibits remarkable enantiofacial selectivity toward nucleophilic attack (Scheme 1B).[7,8]

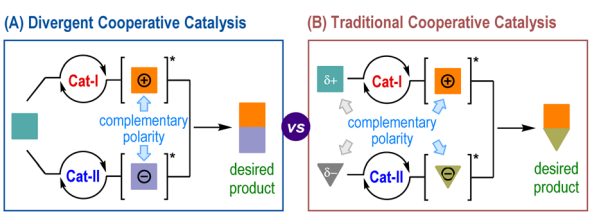

Fig. 1 Conceptual difference between divergent and traditional cooperative catalysis.

Department of Organic Chemistry, Indian Institute of Science, Bangalore 560 012, India. E-mail: sm@iisc.ac.in; Tel: +91-80-2293-2850

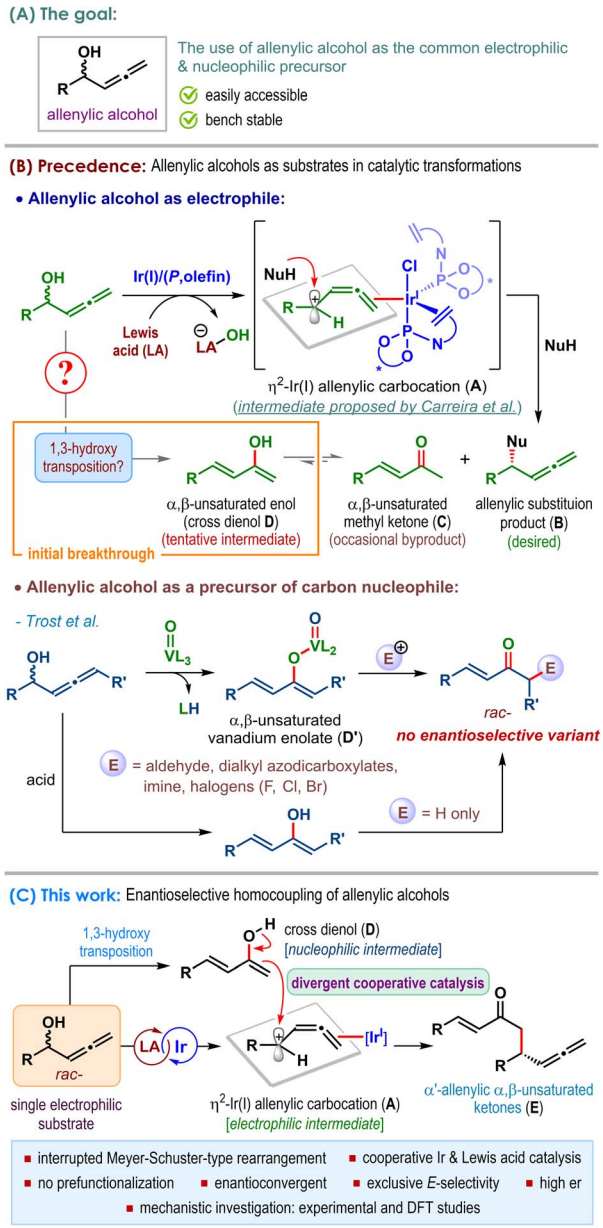

Scheme 1 Allenylic alcohols in divergent cooperative catalysis.

On the other hand, Trost *et al.* elegantly demonstrated the utility of allenylic alcohols as α,β-unsaturated enolate (cross dienolate) precursors.[9] The cross dienolate (**D′**), thus generated through vanadium-catalyzed Meyer–Schuster rearrangement,[10] was trapped with exogenous electrophiles to effect an overall α′-functionalization of α,β-unsaturated ketones (Scheme 1B).[11] In fact, such 1,3-hydroxy transposition in allenylic alcohols is also known to take place under acidic conditions.[12] In all these cases, the traditionally electrophilic allenylic alcohol is converted to nucleophilic cross dienolate without any redox manipulation of the substrate or the catalyst. Similarly, allenylic carbonates have been shown to undergo analogous [3,3]-sigmatropic rearrangement under Lewis acid catalysis.[13] However, to the best of our knowledge such *in situ* generated cross dienols or their derivatives have never been utilized in any enantioselective transformations.

As a part of our ongoing research program dedicated to the development of Ir-catalyzed asymmetric allenylic substitution reactions,[8b–e] we wondered whether the cross dienolate derivatives (*e.g.*, **D** or **D′**) catalytically generated from allenylic alcohols or the corresponding carbonates, can be intercepted with η²-Ir(I)-bound allenylic carbocation intermediate **A** (Scheme 1C). The overall process can be viewed as the homocoupling[14] of allenylic alcohols to generate α′-allenylic α,β-unsaturated ketones **E** without having to use any preformed carbon nucleophile. The compatibility of the two catalyst systems would, of course, be critical to the success of this divergent cooperative catalytic process.

Even though Trost's vanadium-catalyzed Meyer–Schuster rearrangement of allenylic alcohols[9,11] itself constitutes a potential route to cross dienolates, the lack of enantioselective reaction with vanadium dienolate **D′** (Scheme 1B), possibly due to the requirement of harsh reaction conditions, inspired us to seek a milder alternative.

During the asymmetric allenylic substitution of branched allenylic alcohols under Ir(I)/Lewis acid catalysis, the formation of α,β-unsaturated methyl ketone (**C**) as the byproduct is occasionally encountered (Scheme 1B).[8b,c,15] While contemplating the mechanism of its formation, we speculated the intermediacy of cross dienol (**D**), generated through Meyer–Schuster-type 1,3-hydroxy transposition of allenylic alcohols.[16] Although the catalyst responsible for this hydroxy transposition was unclear at this point, the isolation of α,β-unsaturated ketones did serve as the initial breakthrough, at least with respect to the compatibility of the two catalytic processes. Moreover, the known reactivity of the proposed η²-Ir(I) allenylic carbocation **A** towards enol silanes,[7a] extended enol silanes[8b] and even stabilized enols[8c] lends credence to our hypothesis of combining **A** with an *in situ* generated cross dienol **D** as the carbon nucleophile.

However, considering the high reactivity of these two catalytically generated intermediates, the possibility of their competing reactions with other polarity-matched partners could not be underestimated. For example, allenylic alcohol can itself act as an *O*-nucleophile for **A** to produce bis-allenylic ether

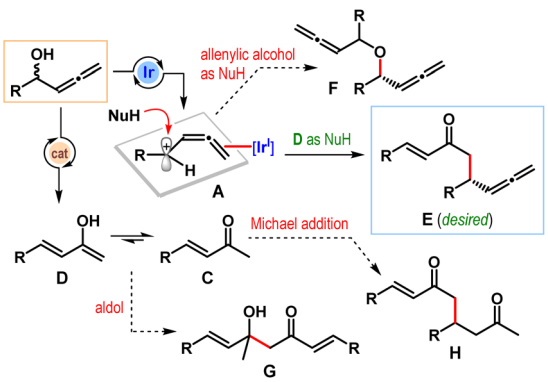

Scheme 2 Potential competing pathways.

F (Scheme 2). Tautomerization of cross dienol **D** to the corresponding α,β-unsaturated methyl ketone **C** can compete with its reaction towards **A**. Similarly, α,β-unsaturated ketone **C** is a potent electrophile and depending on its relative rate of formation, can give rise to aldol or Michael adducts (**G** and **H**, respectively) by reacting with cross dienol **D**. Therefore, minimizing these competing pathways was deemed essential to achieve the desired homocoupling of allenylic alcohols.[17]

Results and discussion

Our initial objective was therefore set to identify the optimum combination of catalysts and reaction conditions to minimize the competing pathways (Scheme 2) and achieve high diastereo- (*E*/*Z*-ratio) and enantioselectivity in this homocoupling of allenylic alcohols. The reaction of racemic allenylic alcohol **1a** in the presence of 6 mol% of an Ir(I)-complex, generated *in situ* from $[Ir(COD)Cl]_2$ and Carreira's (*P*,olefin) ligand[18] (S_a)-**L** in combination with a Lewis acidic promoter was chosen for this purpose (Table 1). Although no reaction took place with 10 mol% of $La(OTf)_3$ as the promoter in THF at 25 °C (Table 1, entry 1), changing the Lewis acid to $Bi(OTf)_3$ resulted in the formation of the desired α′-allenylic α,β-unsaturated ketone **2a**, exclusively as the (*E*)-isomer in only 22% yield but with 99 : 1 er within 10 h (Table 1, entry 2). As anticipated, tautomerization of the hydroxy transposed enol (**D** → **C** in Scheme 2) to benzylidene acetone (**3a**) turned out to be the only competing reaction. The formation of no other byproduct could be detected under these conditions. Even though separable from **2a**, our initial efforts to minimize the formation of enone **3a** and increase the yield of **2a** included the screening of Lewis acidic promoters (Table 1, entries 3–7), which identified $Sc(OTf)_3$ as the optimum. Under these conditions, **2a** was obtained essentially as a single enantiomer in 62% yield (see SI for yield calculation) with an improved **2a**/**3a** ratio of 1 : 1 (Table 1, entry 7). With $Sc(OTf)_3$ as the promoter, screening of solvents revealed the crucial role of reaction medium on the outcome. The use of other ethereal solvents like CPME and TBME favored the formation of **3a** with up to 15 : 1 **3a**/**2a** ratio (Table 1, entries 10 and 11). Clearly tautomerization of the enol is facilitated over its addition to allenylic carbocation in these ethereal solvents. The yield of **2a** remained unaltered when the reaction was carried out at a lower initial concentration of *rac*-**1a** (Table 1, entry 12). Surprisingly, no trace of **2a** or **3a** could be detected when the reaction was carried out in the presence of 4 Å MS under otherwise identical reaction conditions. Instead, bis-allenylic ether **4a** was isolated as the sole product in 51% yield after 36 h as a 1 : 1 *chiral*/*meso* mixture where chiral **4a** was formed with 99.9 : 0.1 er (Table 1, entry 13). The formation of ether **4a** can be explained *via* the nucleophilic attack of allenylic alcohol **1a** to the Ir-bound allenylic carbocation intermediate **A** (Scheme 2). Our attempt to minimize the protonation of cross dienol **D** and enhance its nucleophilicity by using Cs_2CO_3 proved ineffective as *rac*-**1a** was recovered without any trace of **2a** or **3a** (Table 1, entry 14).

Table 1 Optimization of reaction parameters

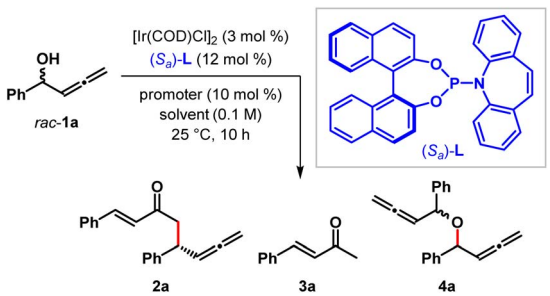

Entry	Promoter	Solvent	**2a**/**3a**	Yield of **2a**[a] (%)	er[b]
1	$La(OTf)_3$	THF	n.d.	<5	n.d.
2	$Bi(OTf)_3$	THF	1 : 3	22	99 : 1
3	$Zn(OTf)_2$	THF	1 : 1.6	28	>99.9 : 0.1
4	$Yb(OTf)_3$	THF	1 : 1.5	47	99.5 : 0.5
5	$Fe(OTf)_2$	THF	1 : 1.6	48	99.9 : 0.1
6	$In(OTf)_3$	THF	1 : 1.7	47	>99.9 : 0.1
7	**$Sc(OTf)_3$**	**THF**	**1 : 1**	**(62)**	**>99.9 : 0.1**
8	$Sc(OTf)_3$	Et_2O	1 : 2.7	40	98 : 2
9	$Sc(OTf)_3$	MeCN	1 : 1.9	52	99 : 1
10	$Sc(OTf)_3$	CPME	1 : 8	17	96 : 4
11	$Sc(OTf)_3$	TBME	1 : 15	11	97 : 3
12[c]	$Sc(OTf)_3$	THF	1 : 1	60	99 : 1
13[d]	$Sc(OTf)_3$	THF	—	(51)[e]	99.9 : 0.1[f]
14[g]	$Sc(OTf)_3$	THF	n.d.	<5	n.d.

[a] Reactions were performed using 0.2 mmol of *rac*-**1a**. Yields were determined by ^1H NMR using mesitylene as internal standard. Isolated yields after chromatographic purification are shown in parentheses. [b] Enantiomeric ratio (er) of **2a**, unless noted otherwise, as determined by HPLC using a stationary phase chiral column. [c] Reaction with 0.05 M initial concentration of *rac*-**1a**. [d] Reaction in the presence of 4 Å MS. [e] Isolated yield of ether **4a** (as 1 : 1 *chiral*/*meso*) after 36 h. [f] Er of chiral **4a**. [g] Reaction in the presence of 1.5 equiv of Cs_2CO_3. n.d. = not determined. CPME = cyclopentyl methyl ether. TBME = *tert*-butyl methyl ether.

While the formation of enone **3a** could not be suppressed, its facile separation from **2a** through silica gel column chromatography allowed us to demonstrate the generality of this enantioselective homocoupling of allenylic alcohols. The conditions shown in entry 7 of Table 1 were applied to a wide range of allenylic alcohols of diverse steric and electronic nature (Table 2). Allenylic alcohols bearing electron-rich aryl substituents were well tolerated to afford α′-allenylic enones **2b–f** and **2i–r** in moderate to good yields with outstanding enantioselectivities. Allenylic alcohols bearing electron-deficient aryl substituents (**1g–h**) failed to deliver the desired products at ambient temperature which points towards the low nucleophilicity of the corresponding cross dienols (**D** in Scheme 1C). However, these reactions took place at 50 °C and resulted in the formation of the α′-allenylic enones (**2g–h**) in low yields but with excellent enantioselectivities. Allenylic alcohols, having polyaromatic hydrocarbon, delivered the products (**2n–q**) in moderate to good yields while excellent enantioselectivities were maintained. Heterocyclic substituents such as 1,3-benzodioxole (**1r**) thiophene (**1s–t**) and furan (**1u**) on allenylic alcohols were found to be compatible with our standard reaction conditions and furnished the corresponding products **2r–u** in decent yields with excellent er (up to >99.9 : 0.1). To our delight, 1-cyclopropyl allenylic alcohol **1v** afforded the desired

Table 2 Substrate scope[a]

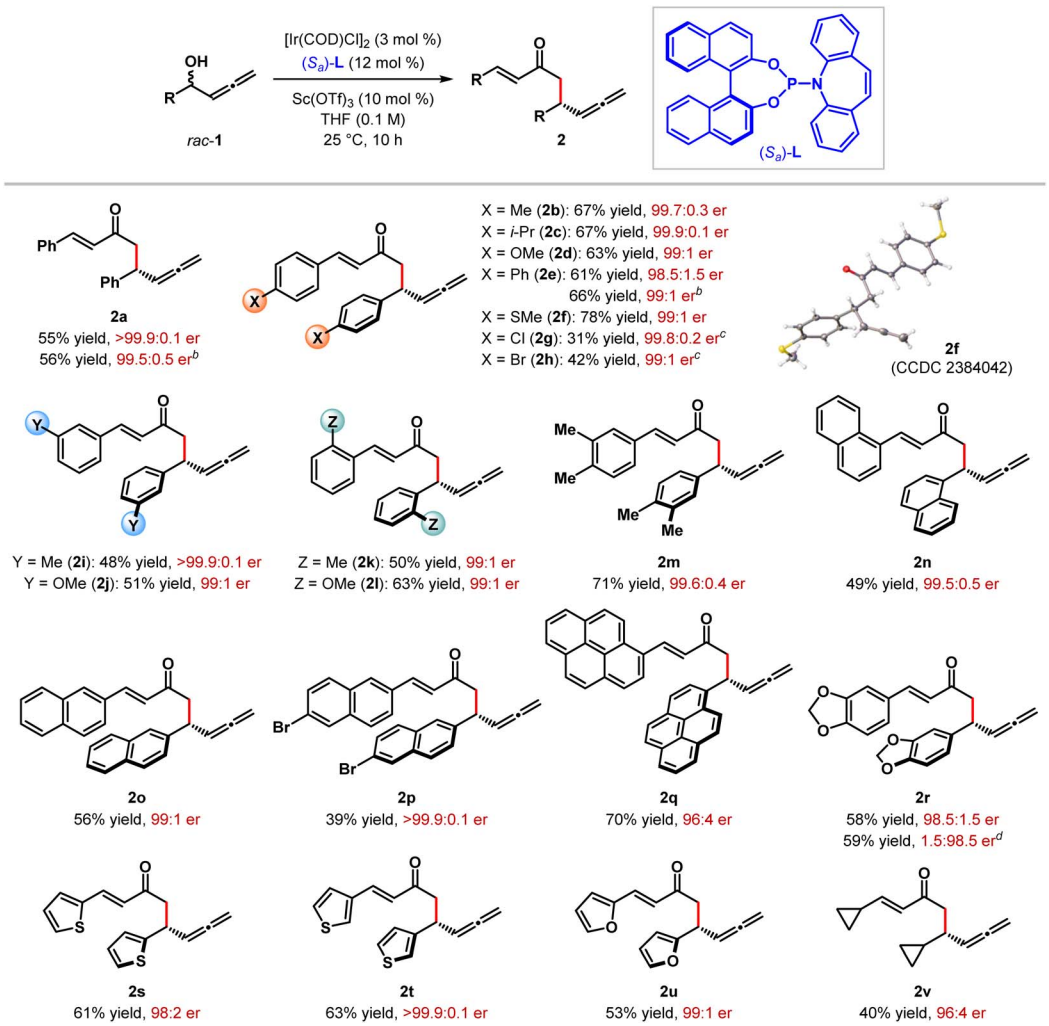

[a] Unless stated otherwise, the reactions were carried out using 0.4 mmol of *rac*-**1**. Yields correspond to the isolated yield after chromatographic purification. Enantiomeric ratios (er) were determined by HPLC analysis using stationary phase chiral columns. [b] Reaction using 2.0 mmol of *rac*-**1**. [c] Reaction at 50 °C. [d] Reaction using 5.8 mmol of *rac*-**1r** and 2 mol% Ir(I)/(R_a)-**L** complex.

product **2v** with 96 : 4 er, albeit in only 40% yield. It must be noted that in all these cases the desired α′-allenylic enones were obtained exclusively as a single diastereomer (>20 : 1 *E*/*Z*).

The limitations of our protocol include low to moderate yields and incompatibility of electron-deficient as well as aliphatic allenylic alcohols. Aliphatic allenylic alcohols failed to participate in this homocoupling reaction, possibly due to the lack of stability of the corresponding allenylic carbocation. The incompatibility of aliphatic allenylic alcohol in allenylic substitution is a known limitation of this catalyst system. The low product yields in some of the cases can be attributed to competing tautomerization of the cross dienols to the corresponding enones. Similarly, tertiary allenylic alcohols also failed to participate in this homocoupling process and only resulted in enones.

The reaction scaled well, as exemplified with **2a**, **2e**, and **2r**. In the last case, the loading of the Ir(I)/(R_a)-**L** complex could be reduced to 2 mol% without any effect on either yield or enantioselectivity (Table 2).

The absolute configuration of α′-allenylic enone **2f** was established by single crystal X-ray diffraction analysis (CCDC 2384042) and found to be (*R*). The absolute stereochemistry of other α′-allenylic enones was tentatively assigned the same by analogy.

The synthetic utility of densely functionalized α′-allenylic enones was illustrated through a variety of synthetic elaborations (Scheme 3). For example, Luche reduction followed by dehydration under acidic conditions transformed **2a** into skipped diene-allene **5** in 51% yield with 3 : 1 dr with respect to the newly formed olefin. Exposure of **5** to hydrogen and Pd/C in MeOH resulted in enantioenriched hydrocarbon **6**, bearing an "orphaned" stereocenter,[8b] in excellent yield. The enantioselective synthesis of such a saturated hydrocarbon would be otherwise challenging. Conjugate addition of $Ph_2CuMgBr$[19] to

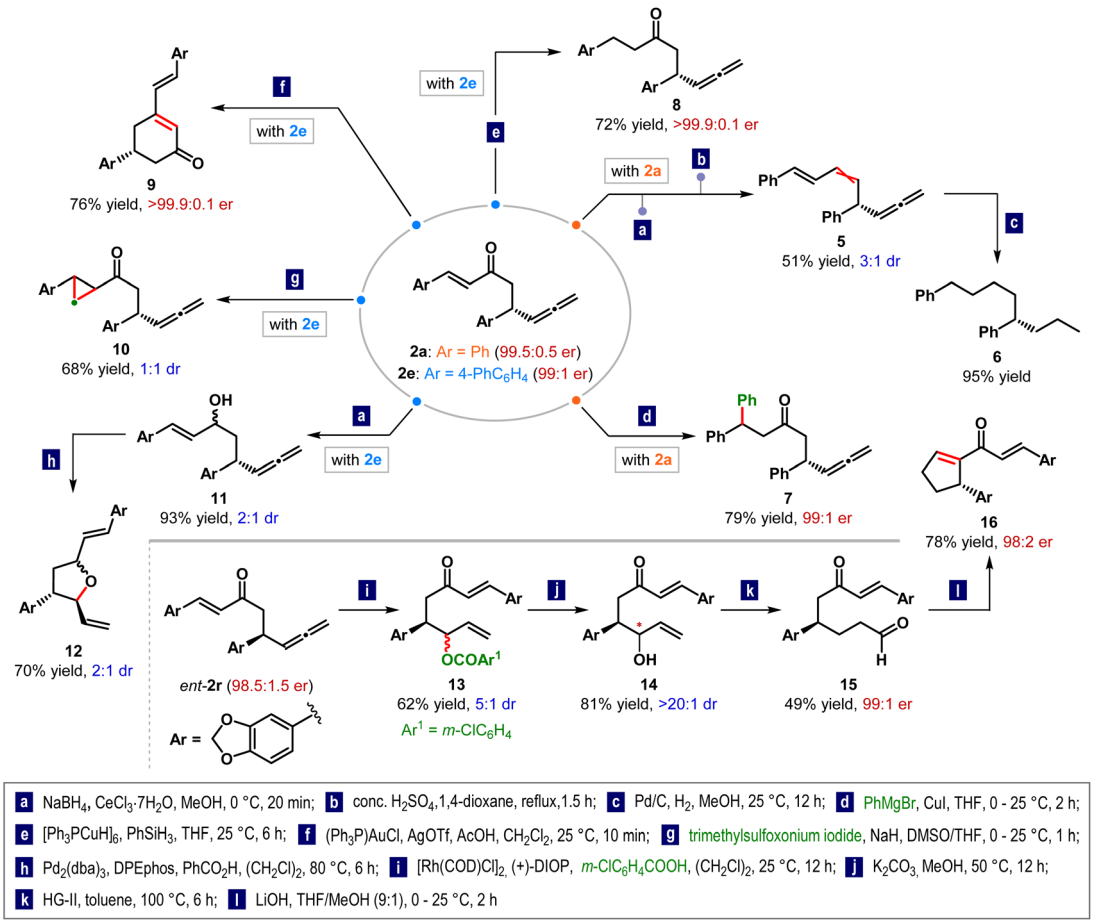

Scheme 3 Synthetic elaboration of α′-allenylic enones.

2a furnished β,β-disubstituted ketone **7** in 79% yield. Selective reduction of the electron-deficient olefin in **2e** using Stryker's reagent[20] led to the formation of ketone **8** in 72% yield. Au-Catalyzed hydration/intramolecular aldol condensation cascade[8e] of **2e** afforded enantiopure cyclohexenone **9**, bearing a δ-stereocenter, in 76% yield. Corey-Chaykovsky cyclopropanation[21] of **2e** took place without any diastereocontrol as the corresponding α,β-cyclopropyl ketone **10** was formed with 1 : 1 dr in 68% yield. Allylic alcohol **11**, prepared by Luche reduction of **2e**, when subjected to Pd-catalyzed intramolecular hydroalkoxylation[22] of allene, led to the formation of 1,2,4-trisubstituted tetrahydrofuran **12** in 70% yield with modest dr. However, during this cyclization, the newly formed stereocenter was generated exclusively in *trans*-fashion with respect to the adjacent stereocenter.

Rh-Catalyzed hydrocarboxylation[14e] of allene in *ent*-**2r** delivered allylic benzoate **13**, bearing two vicinal stereogenic centers, in 62% yield with 5 : 1 dr. Hydrolysis of benzoate in **13** afforded allylic alcohol **14**, which could be isolated as a single diastereomer in 81% yield after column chromatographic purification. Our attempted ring-closing metathesis of **14** under Hoveyda–Grubbs 2nd generation catalyst (HG-II) converted the allylic alcohol into aldehyde **15** through a hydroxy transposition/isomerization/tautomerization cascade.[23] The presence of a 1,6-dicarbonyl functionality in **15** made it an eligible candidate for intramolecular aldol condensation. When exposed to LiOH in THF/MeOH, **15** indeed underwent annulation to generate cyclopentene **16** in 78% yield with reduced er.

To shed light on the mechanism of this homocoupling of allenylic alcohols, we undertook a detailed investigation of each step of this reaction pathway.

In this direction, we first focused on the 1,3-hydroxy transposition of allenylic alcohol to cross dienol **D** (Scheme 1B). This hydroxy transposition reaction was found to take place efficiently in the absence of the Ir(I)/(S_a)-**L** complex, as only 10 mol% of $Sc(OTf)_3$ converted *rac*-**1a** into (*E*)-**3a** in 71% yield in THF at 25 °C within 48 h (Scheme 4A). Clearly, iridium does not play any role in this hydroxy transposition reaction. Under the same reaction conditions, tertiary allenylic alcohol **1w** also gave rise to the corresponding (*E*)-enone **3w**, exclusively, in 76% yield. However, this hydroxy transposition of **1a** is sluggish at 10 °C, as only 9% of **3a** could be isolated after 48 h. Similarly, in the presence of 4 Å MS, **1a** remained unreacted and no **3a** could be detected. The inhibition of 1,3-hydroxy transposition pathway in the presence of 4 Å MS explains the obstruction of the coupling reaction (Table 1, entry 13) and highlights the role of adventitious water in this hydroxy transposition.

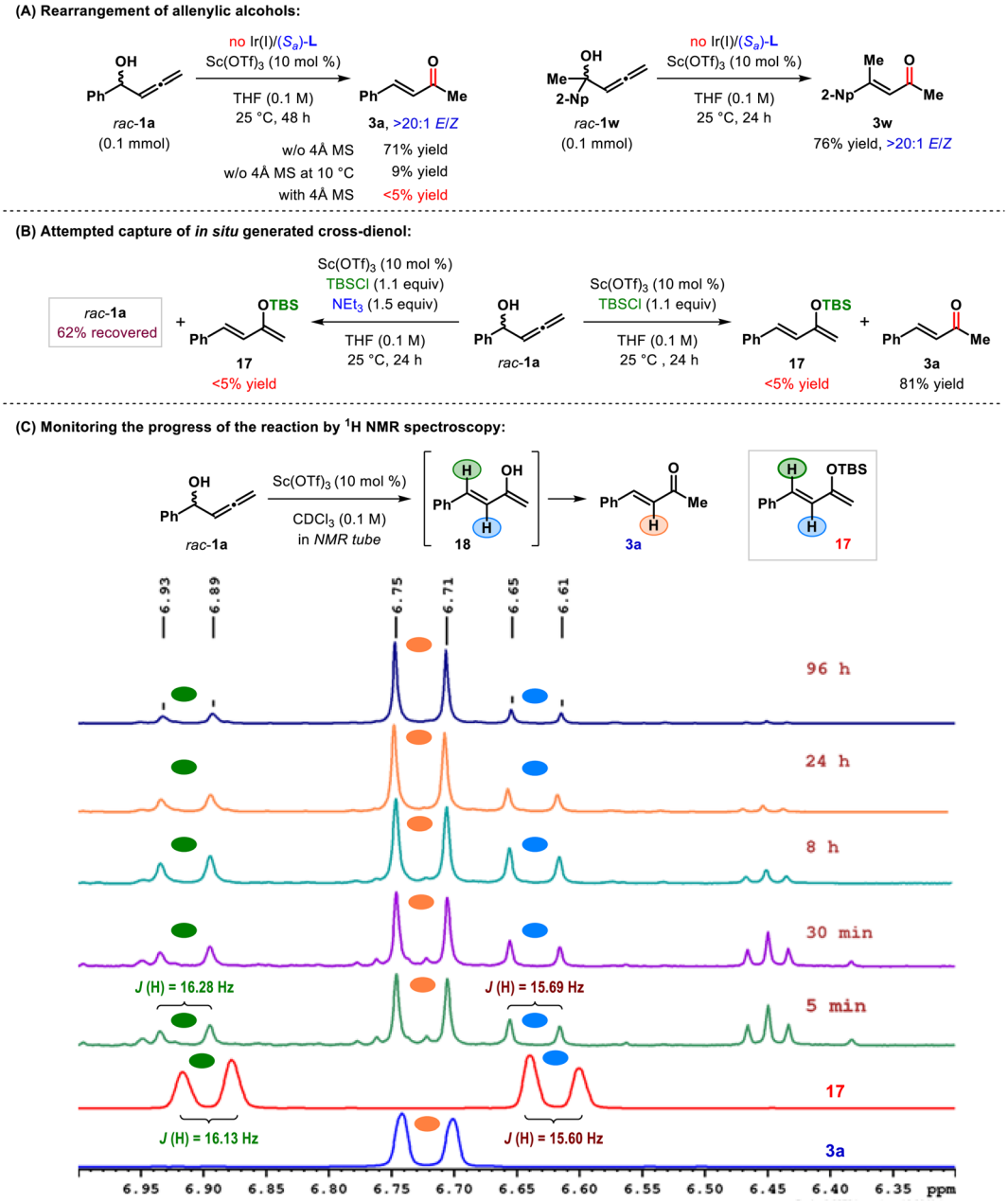

Scheme 4 Control experiments and ^{1}H NMR analysis of 1,3-hydroxy transposition of allenylic alcohols.

Our efforts in capturing the cross dienol generated *in situ* from *rac*-**1a** as its silyl ether **17** proved futile since its tautomerization to **3a** was found to be faster than *O*-silylation (Scheme 4B). An attempted facilitation of *O*-silylation through the addition of a base (NEt_3) completely suppressed the 1,3-hydroxy transposition and led to the recovery of *rac*-**1a**. This outcome underscores the requirement of an acidic environment for hydroxy transposition.

Even though we failed to capture the cross dienol **18** as its silyl enol ether **17**, it was possible to detect its formation by monitoring the progress of the reaction by ^{1}H NMR spectroscopy. Apart from the characteristic signals of *rac*-**1a** and **3a**, two new doublets at 6.91 ppm (J = 16.3 Hz) and 6.63 (J = 15.7 Hz) appeared within 5 min of the addition of 10 mol% $Sc(OTf)_3$ to a solution of *rac*-**1a** in $CDCl_3$ at 25 °C (Scheme 4C). These signals persisted even after 96 h. By comparing the chemical shifts and coupling constants with preformed silyl dienol ether **17**, the spectroscopic signature of these two doublets was reasonably established. The slight downfield shift of these two olefinic proton signals of **18** compared to those in **17** stems from the difference in their electronic environment due to the presence of the TBS group and is in agreement with the literature.[24] The exclusive formation of (*E*)-configured cross dienol in this reaction is particularly noteworthy.

To study the role of external water in the hydroxy transposition reaction, we carried out a series of isotope-labelling

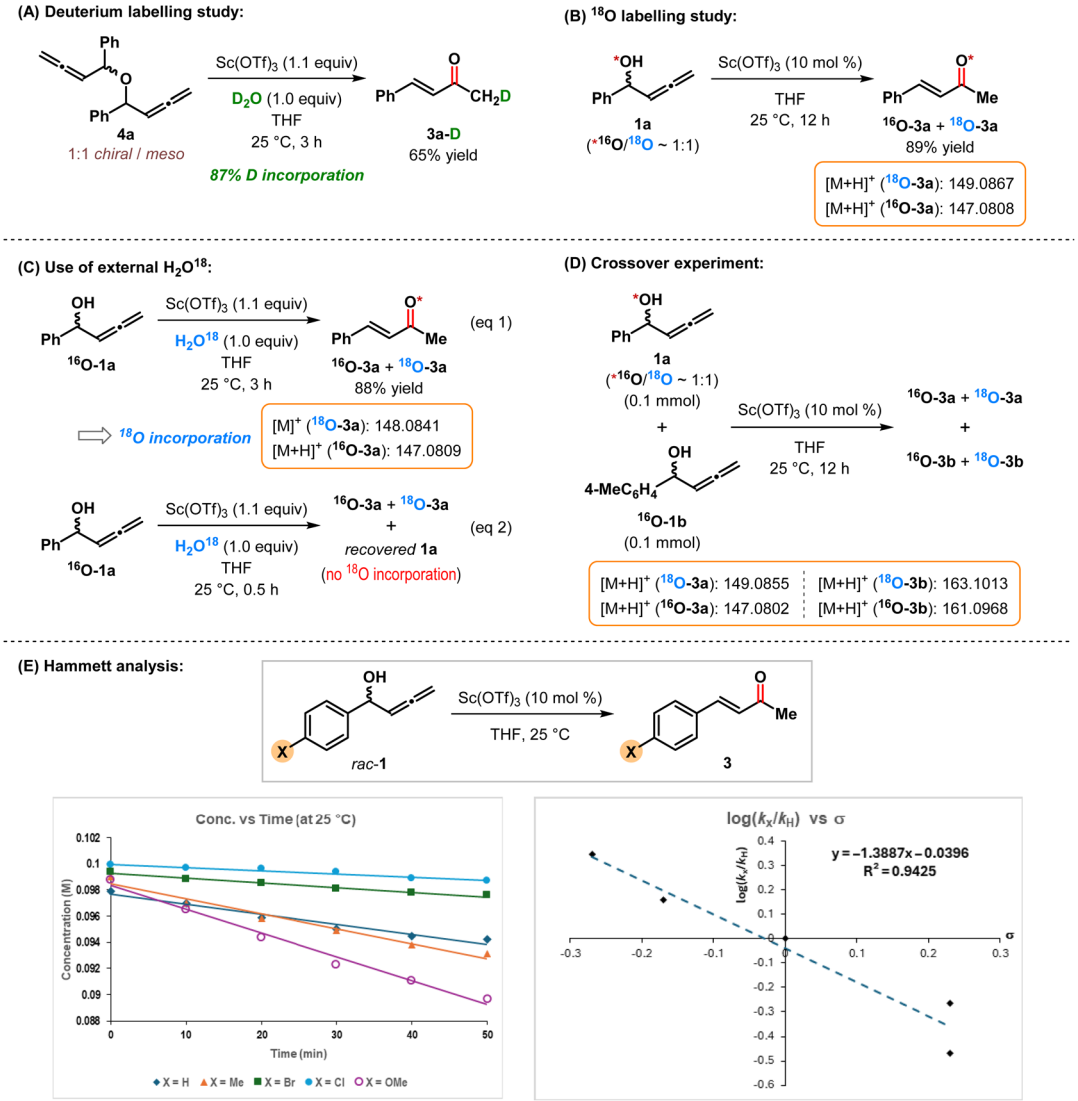

Scheme 5 Isotope labelling study and Hammett analysis of 1,3-hydroxy transposition of allenylic alcohols.

experiments. Formation of bis-allenylic ether **4a** was observed in the Ir-catalyzed reaction of **1a**, when carried out in the presence of 4 Å MS (Table 1, entry 13). We wondered whether **4a** can be transformed into cross dienol in the presence of external water. When treated with $Sc(OTf)_3$ in THF in the presence of 1.0 equiv of D_2O, **4a** was indeed transformed into monodeuteriated benzylidene acetone **3a-D** (Scheme 5A). The incorporation of 87% D only at the α-position of **3a-D** further confirms the intermediacy of cross dienol (**18**) in this reaction.

When the transposition of a nearly equimolar mixture of ^{16}O-**1a** and ^{18}O-**1a** was allowed to take place, ^{18}O was found in **3a**, which indicates that the source of oxygen in benzylidene acetone is the parent allenylic alcohol **1a** (Scheme 5B). However, ^{18}O incorporation also took place when external H_2O^{18} was used in combination with ^{16}O-**1a** (Scheme 5C, eqn (1)). The outcome of this experiment shows that the hydroxy transposition may not necessarily be intramolecular in nature. To ascertain the likelihood of an intermolecular pathway, we analyzed the same reaction before completion (Scheme 5C, eqn (2)). No exchange with ^{18}O in the recovered allenylic alcohol **1a** was detected. Clearly the initial hydroxy dissociation step is irreversible in nature and ^{18}O-**3a** arises from the direct reaction with H_2O.[18] To further probe the nature of the hydroxy transposition step, a crossover experiment was conducted: An equimolar mixture of **1b** and ^{18}O-labeled **1a** ($^{16}O/^{18}O \sim 1:1$) was stirred in THF at 25 °C in the presence of 10 mol% $Sc(OTf)_3$ for 12 h (Scheme 5D). The formation of ^{18}O-**3b**, as detected by HRMS analysis, confirms that the hydroxy transposition of allenylic alcohol is intermolecular in nature and eliminates the possibility of a Lewis acid-assisted concerted intramolecular migration of the hydroxy group through a four-membered transition state. Therefore, a Lewis acid-assisted hydroxy dissociation from allenylic alcohol and subsequent rebound of the hydroxy group with the allenylic carbocation at the erstwhile sp-hybridized carbon appears to be the likely pathway (*vide infra*).

To understand the nature of the intermediate in this hydroxy transposition reaction, a linear free-energy relationship (LFER) study was conducted using allenylic alcohols bearing different

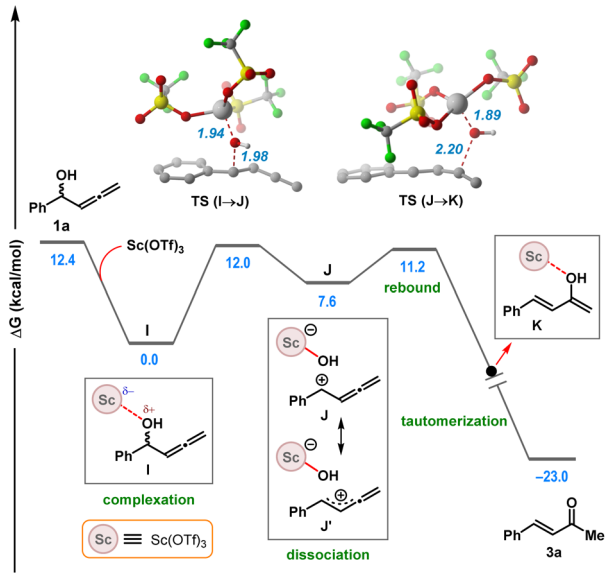

Fig. 2 Free energy profile diagram for the hydroxy transposition reaction of allenylic alcohol **1a** using $Sc(OTf)_3$. Energies are reported in kcal mol^{-1}. The values in parentheses refer to electronic energies. Distances are in Å. Hydrogen atoms are omitted for clarity.

para-substituted aryl groups (Scheme 5E). The plot of the Hammett substituent constants (σ)[25] *vs.* $\log(k_X/k_H)$ revealed a linear correlation with a moderately negative slope ($\rho = -1.39$), which implies positive charge buildup in the rate-limiting transition state and is consistent with an S_N1-type ionization step. We also considered an S_N2' pathway for this hydroxy transposition. However, control experiments with external nucleophiles (see SI) eliminate this possibility.

In order to support this proposition further, density functional theory (DFT) calculations were performed for the reaction of allenylic alcohol **1a** using $Sc(OTf)_3$ as the Lewis acid.

Due to the high oxophilicity of $Sc(OTf)_3$, the formation of the adduct **I** is facilitated (Fig. 2). Subsequent ionization of the Sc(III)-activated hydroxy group *via* **TS** (**I** → **J**) results in a loosely bound ion-pair intermediate **J**. Natural population analysis

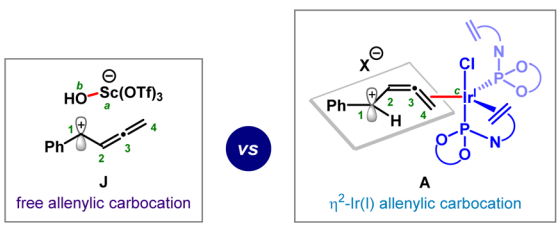

species	charge center		
	a	1	3
I	+0.642	+0.140	+0.086
TS (I→J)	+0.621	−0.113	+0.306
J	+0.694	−0.058	+0.334
A	-	+0.325	+0.277

Fig. 3 NPA charge analysis.

(NPA)[26] of charge for this dissociation step confirmed the carbocationic character of the transition state **TS** (**I** → **J**) and the intermediate **J** with a decreased electron density at the C3 position of **J** compared to that in **I** (Fig. 3). This enhanced positive charge at C3 is responsible for the site-selective rebound of the hydroxy group at C3 and accounts for the irreversibility of the initial hydroxy dissociation step (*i.e.*, unfavorable rebound at C1). The DFT calculations also revealed a low barrier (3.6 kcal mol^{-1}) for this hydroxy rebound step [*via* **TS** (**J** → **K**)] to the enol intermediate **K**. Similarly, the attack of external nucleophiles is restricted solely to the C3 position of the free carbocation.

This site selectivity comes in stark contrast to the Ir(I)-bound allenylic carbocation **A**, which favors nucleophilic attack at the C1 position (Fig. 3).[7c,d] NPA charge analysis on **A** also reveals a strong carbocationic character at its C1 position (see SI). This preferential behavior of **A** can be attributed to the direct interaction between the electron-rich iridium center and the delocalized positively charged π-accepting substrate. The π-back donation occurs from a suitably oriented orbital of iridium to the allenylic carbocation. This metal coordination not only redefines the potential electrophilic site from C3 to C1 but also, through the presence of the chiral ligand attached to iridium, which impedes nucleophilic attack at the C3 position owing to steric crowding (*vide infra*).

Subsequent tautomerization of **K** furnishes enone **3a** (Fig. 2). This tautomerization step was found to be assisted by external water molecules and allenylic alcohol **1a**, since the direct proton transfer has a prohibitively high activation barrier (see SI). DFT studies corroborated the experimental findings wherein the rate-determining step of the hydroxy transposition reaction was implied to be an S_N1 type ionization, ultimately forming an ion-pair intermediate that can easily undergo crossover reactions (Scheme 5D). Our efforts to locate a transition state for an alternative pathway involving Lewis acid-assisted concerted intramolecular migration of the hydroxy group through a four-membered transition state remain unsuccessful.

With a reasonably clear mechanistic picture of the 1,3-hydroxy transposition of allenylic alcohol (*e.g.*, **1a**) to cross dienol **18** (Scheme 4C), we turned our attention to the allenylic substitution step.

During the optimization study, bis-allenylic ether **4a** was obtained as the only product when the reaction was carried out in the presence of 4 Å MS (Table 1, entry 13). The formation of **4a** can be rationalized by the nucleophilic addition of allenylic alcohol (*rac*-**1a**) to the Ir-bound allenylic carbocation **A** (Scheme 2) in the absence of any other nucleophile. Since hydroxy transposition in allenylic alcohol does not take place in the presence of 4 Å MS (Scheme 4A), ether **4a** emerged as the sole product. This C–O bond formation between *rac*-**1a** and **A** can be expected to be enantioselective, which accounts for the *chiral*/*meso* ratio (1 : 1) of **4a** and high enantioselectivity (99.9 : 0.1 er) of *chiral*-**4a**.

We were curious about the intermediacy of bis-allenylic ether (*e.g.*, **4a**) in this homocoupling reaction, leading to α′-allenylic enones. In a preparative experiment, **4a** was isolated in 82% yield after 72 h using 4 Å MS as an additive under otherwise

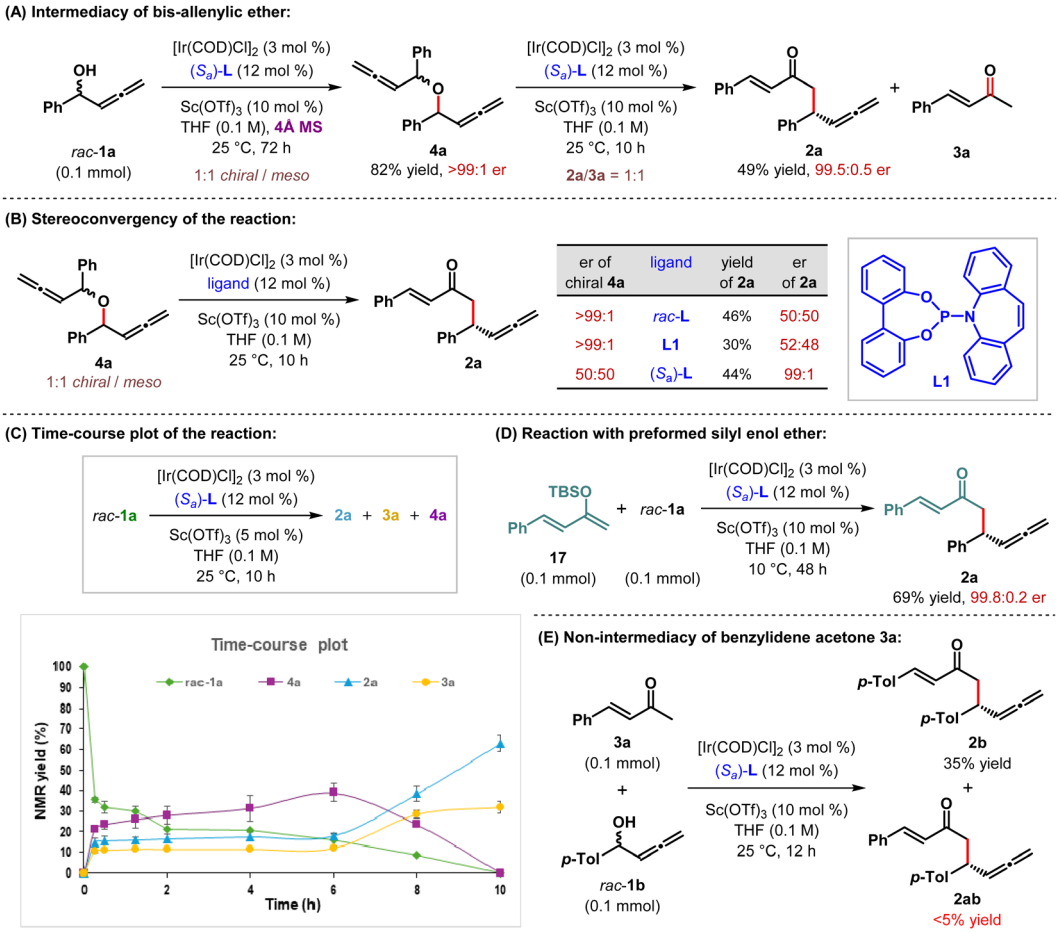

Scheme 6 Control experiments and reaction profile.

optimized reaction conditions (Scheme 6A). When **4a** was subjected to the standard coupling conditions (*i.e.*, without 4 Å MS), **2a** was isolated in 49% yield with a similar level of enantioselectivity while maintaining a similar **2a**/**3a** ratio. Therefore, bis-allenylic ether **4a** can be considered as an intermediate which is eventually converted to **2a** and **3a**.

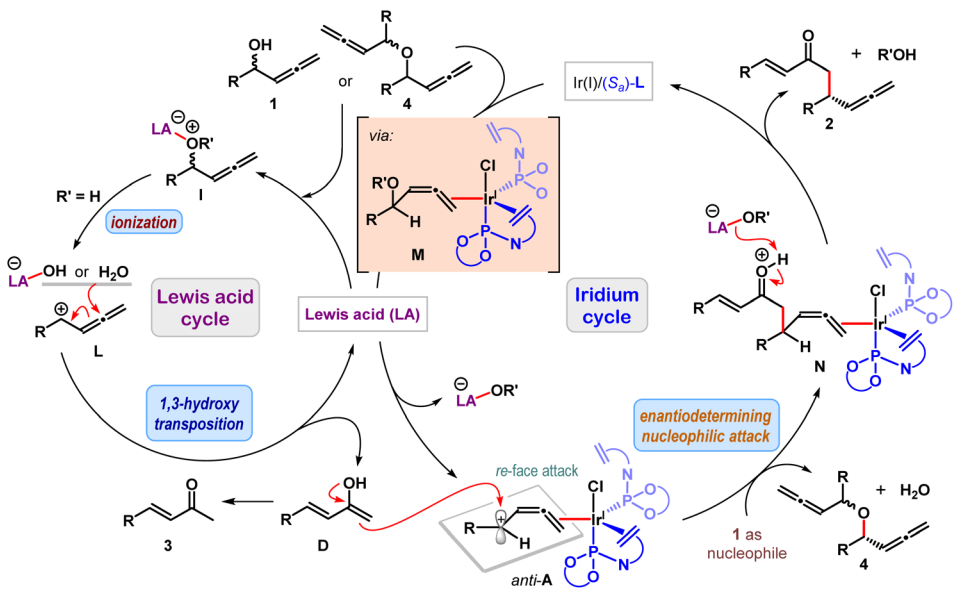

Scheme 7 A plausible divergent cooperative catalytic cycle for the homocoupling of branched allenylic alcohol.

When a 1 : 1 mixture of *meso*-**4a** and enantiopure **4a** was subjected to the coupling reaction using either racemic or achiral (*P*,olefin) ligands (*rac*-**L** or **L1**, respectively), α′-allenylic enone **2a** was obtained as racemate (Scheme 6B). Conversely, **2a** was isolated with excellent er when the mixture of racemic and *meso*-**4a** was employed as substrate under (S_a)-**L**. These observations confirm complete catalyst control and the stereoconvergency of the process.

A time-course analysis of this homocoupling reaction (Scheme 6C) revealed rapid initial depletion of *rac*-**1a** (within 15 min) along with simultaneous formation of **2a**, **3a** and **4a** in considerable amounts. Subsequent consumption of *rac*-**1a** leads to the formation of **4a** predominately, with a minimal increase in the amount of **2a** and **3a** up to 6 h. Finally, the disappearance of **4a** results in **2a** and **3a**. Due to the low initial concentration of the *in situ* generated cross dienol at the early phase of the reaction, allenylic alcohol **1a** outweighs it as the nucleophile and generates bis-allenylic ether **4a**, which acts as an alternative substrate. As the reaction proceeds, appearance of cross dienol (either from **1a** or from **4a**) gives rise to **2a** along with its tautomerization to **3a**. Overall, this kinetic profile resembles that of a consecutive reaction.[27]

The allenylic substitution of *rac*-**1a** with preformed silyl enol ether **17** under our otherwise standard catalytic conditions at 10 °C resulted in 69% of α′-allenylic enone **2a** with 99.8 : 0.2 er (Scheme 6D). Since the hydroxy transposition takes place very slowly at 10 °C (see Scheme 4A), the formation of **2a** can be explained as the outcome of the reaction between **17** and **1a** instead of the homocoupling of **1a**. In fact, an attempted coupling reaction of **1a** at 10 °C proved ineffective as the formation of only 20% of bis-allenylic ether **4a** was observed without any trace of **2a** or **3a** (see SI). The generation of **2a** from **17** with the same sense of enantioinduction and the similar level of er confirms the intermediacy of cross dienol **D** as an intermediate in this reaction.

To check the potential intermediacy of benzylidene acetone **3a** in this reaction, a 1 : 1 mixture of **3a** and *rac*-**1b** was subjected to our standard reaction conditions (Scheme 6E). Although homocoupling product of **1b** (*i.e.*, **2b**) was formed in 35% yield, no trace of the cross-coupled product **2ab** could be detected. Clearly, **3a** is not a substrate in this reaction as it does not undergo enolization under our standard conditions. Therefore, the intermediacy of benzylidene acetone (*e.g.*, **3a**) in this reaction can be safely eliminated.

Finally, a reaction between two different allenylic alcohols having similar electronics led to the formation of all four possible α′-allenylic enones (see SI). On the other hand, an attempted cross-coupling between two electronically different allenylic alcohols selectively yielded the homocoupled product of the electron-rich allenylic alcohol. Neither the homocoupling of the electron-deficient counterpart nor any cross-coupled products were detected. The outcome from this experiment indirectly supports the involvement of a carbocation intermediate in this reaction (see SI). Overall, our present catalytic conditions are not suitable for selective cross-coupling of allenylic alcohols.

Based on the information gathered from the above-mentioned control experiments, DFT studies, and prior literature reports,[7c,d,8d,e] a plausible catalytic cycle is conceived. As depicted in Scheme 7, the reaction begins with the Lewis acid (LA) assisted irreversible ionization of allenylic alcohol **1** to generate the free allenylic carbocation **L**. Nucleophilic attack from LA-bound hydroxy group or external water to **L** results in an overall 1,3-hydroxy transposition of allenylic alcohol to

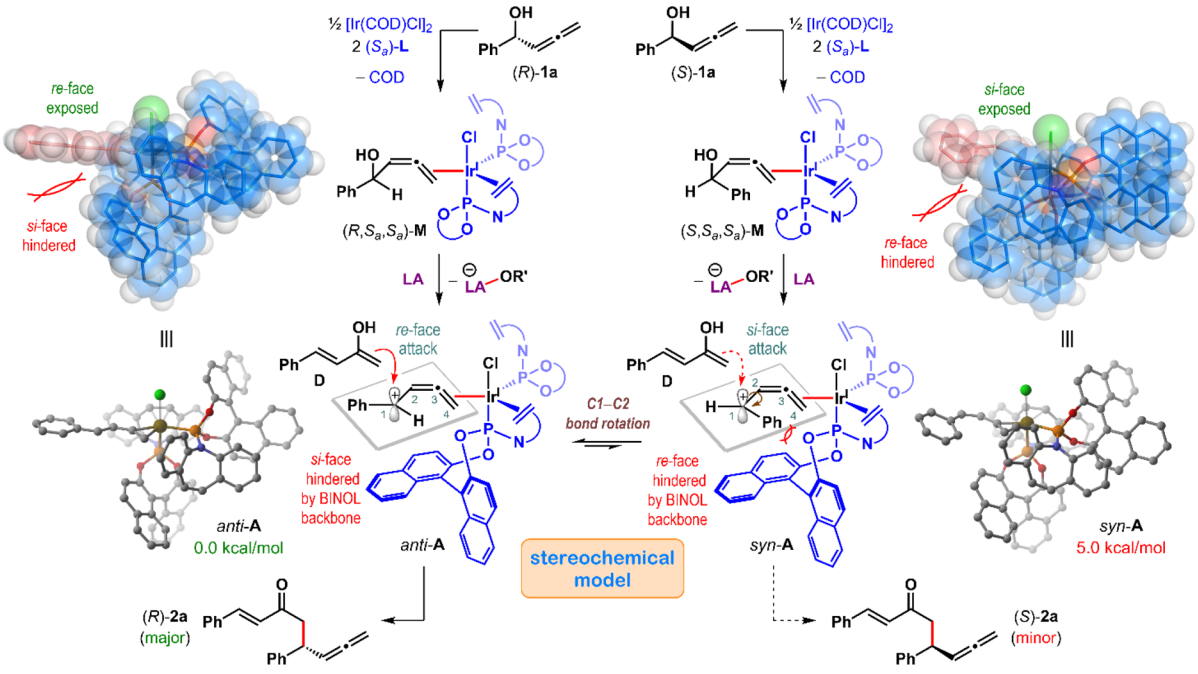

Scheme 8 Proposed stereochemical model for the enantioselective homocoupling of branched allenylic alcohol.

deliver the cross dienol intermediate **D**. In the iridium cycle, LA activation of the (η^2-allenylic alcohol)Ir(I) **M** followed by ionization results in the formation of the putative Ir(I)-bound allenylic carbocation **A**.[7d]

Allenylic carbocation **A** can be generated in *anti* or *syn* fashion (Scheme 8). The formation of these Ir(I)-bound *anti*- and *syn*-butadienylium cations directly reflects the stereochemical information transferred from the allenylic alcohol **1** or bis-allenylic ether **4**. In *anti*-**A**, the *si*-face (bottom face) of the planar butadienylium cation is sterically blocked by the binaphthyl group of the axially coordinated (*P*,olefin) ligand on the Ir center (Scheme 8). As a result, the enantioselective nucleophilic addition of cross dienol (**D**) at C1 can only occur from the less hindered *re*-face of *anti*-**A** (Scheme 8), leading to the formation of (*R*)-**2a**.

In contrast, *syn*-**A** is significantly more congested due to the proximity of the phenyl group to the axially coordinated (*P*,olefin) ligand on Ir and destabilized by 5.0 kcal mol^{-1} compared to *anti*-**A** (Scheme 8). This increased steric hindrance renders nucleophilic attack of **D** on *syn*-**A** energetically less favourable. However, the nucleophilic attack of **D** to the *si*-face of *syn*-**A** is responsible for the formation of the minor enantiomer (*S*)-**2a**. In the absence of any nucleophile, Ir(I)-bound allenylic carbocation **A** is trapped by allenylic alcohol **1** to produce bis-allenylic ether **4**, which also acts as a competent substrate for both the catalytic cycles (Scheme 7). Tautomerization of dienol **D** is a competing pathway and results in enone **3** as an unavoidable off-cycle byproduct.

Conclusions

In conclusion, we have developed an enantioselective homocoupling of branched allenylic alcohols. Catalyzed cooperatively by an Ir(I)/(phosphoramidite,olefin) complex and Lewis acidic $Sc(OTf)_3$, the overall process combines a Meyer–Schuster-type 1,3-hydroxy transposition of allenylic alcohols with enantioselective allenylic substitution. While the transformation of allenylic alcohol to nucleophilic cross dienol takes place solely under Lewis acid catalysis, the conversion of allenylic alcohol to putative η^2-Ir(I)-bound allenylic carbocation transpires under combined Ir(I) and Lewis acid catalysis. Ultimately, the enantioface-selective interception of allenylic carbocation with cross dienol delivers α'-allenylic α,β-unsaturated ketones in moderate to good yields generally with excellent enantioselectivity. This strategy may be termed as *divergent cooperative catalysis*, where a single substrate is converted into two transient intermediates of complementary polarity under the influence of two different catalysts. The selective coupling of these two polarity-matched intermediates results in the desired product. Mechanistic investigations through experimental as well as DFT studies revealed the details of the hydroxy transposition step as well as the origin of enantioselectivity in the allenylation step. This divergent cooperative catalysis strategy benefits from the employment of a single substrate and avoids the use of preformed carbon nucleophiles.

From the conceptual viewpoint, the study presented herein establishes the possibility of designing coupling reactions using a single substrate under redox-neutral conditions. Identification of suitable ambiphilic substrates along with compatible catalyst combinations should see the discovery of new reactions under divergent cooperative catalysis. Moreover, the combination of 1,3-hydroxy transposition of allenylic alcohols with other electrophilic partners can result in cross-electrophilic coupling reactions. Efforts in these directions are currently underway in our laboratory.

Author contributions

A. C. and S. M. conceived and designed the project. A. C. performed the experiments and analyzed the data. R. C. carried out the density functional theory (DFT) studies. The manuscript was written through the contribution of all the authors. All authors approved the final version of the manuscript.

Conflicts of interest

There are no conflicts to declare.

Data availability

CCDC 2384042 contains the supplementary crystallographic data for this paper.[28]

Supplementary information: experimental details, characterization, and analytical data. See DOI: **https://doi.org/10.1039/d5sc02831k**.

Acknowledgements

The funding from Science and Engineering Research Board (SERB), New Delhi in the form of the Science and Technology Award for Research (SERB-STAR) [Grant No. STR/2021/000009] is gratefully acknowledged. A. C. and R. C. acknowledge the Ministry of Education, Government of India for their doctoral fellowships through the Prime Minister's Research Fellowship (PMRF) scheme. The authors' sincere thanks are due to Prof. Garima Jindal (Department of Organic Chemistry, IISc, Bangalore) for helpful discussions. We thank Mr Pankaj Roy for his help with the Hammett analysis and Mr Kishorkumar Sindogi (Central X-Ray Facility, IISc Bangalore) for his help with the X-ray diffraction analysis. We thank Mr Arko Seal for his experimental help during the revision stage of the manuscript. High resolution mass spectra (HR-MS) were recorded on equipment procured under the Department of Science and Technology (DST)-FIST grant [Grant No. SR/FST/CS II-040/2015].

Notes and references

1 (*a*) D. Chaudhary and R. K. Saunthwal, *Org. Chem. Front.*, 2025, **12**, 2025–2051; (*b*) X. Huo, G. Li, X. Wang and W. Zhang, *Angew. Chem., Int. Ed.*, 2022, **61**, e202210086; (*c*) D.-S. Kim, W.-J. Park and C.-H. Jun, *Chem. Rev.*, 2017, **117**, 8977–9015; (*d*) J. Fu, X. Huo, B. Li and W. Zhang, *Org. Biomol. Chem.*, 2017, **15**, 9747–9759; (*e*) S. M. Inamdar, V. S. Shinde and N. T. Patil, *Org. Biomol. Chem.*, 2015, **13**,

8116–8162; (*f*) G. Jindal, H. K. Kisan and R. B. Sunoj, *ACS Catal.*, 2015, **5**, 480–503; (*g*) Z. Du and Z. Shao, *Chem. Soc. Rev.*, 2013, **42**, 1337–1378; (*h*) A. E. Allen and D. W. C. MacMillan, *Chem. Sci.*, 2012, **3**, 633–658.

2 S. Das, B. Mitschke, C. K. De, I. Harden, G. Bistoni and B. List, *Nat. Catal.*, 2021, **4**, 1043–1049.

3 (*a*) L. E. Ehehalt, O. M. Beleh, I. C. Priest, J. M. Mouat, A. K. Olszewski, B. N. Ahern, A. R. Cruz, B. K. Chi, A. J. Castro, K. Kang, J. Wang and D. J. Weix, *Chem. Rev.*, 2024, **124**, 13397–13569; (*b*) K. E. Poremba, S. E. Dibrell and S. E. Reisman, *ACS Catal.*, 2020, **10**, 8237–8246; (*c*) D. A. Everson and D. J. Weix, *J. Org. Chem.*, 2014, **79**, 4793–4798; (*d*) C. E. I. Knappke, S. Grupe, D. Gärtner, M. Corpet, C. Gosmini and A. Jacobi von Wangelin, *Chem.–Eur. J.*, 2014, **20**, 6828–6842; (*e*) Y. Lan, Q. Han, P. Liao, R. Chen, F. Fan, X. Zhao and W. Liu, *J. Am. Chem. Soc.*, 2024, **146**, 25426–25432; (*f*) J. Zhou, D. Wang, W. Xu, Z. Hu and T. Xu, *J. Am. Chem. Soc.*, 2023, **145**, 2081–2087.

4 T. Newhouse, P. S. Baran and R. W. Hoffmann, *Chem. Soc. Rev.*, 2009, **38**, 3010–3021.

5 A. Chakrabarty, R. Chatterjee and S. Mukherjee, Enantioselective Redox-Neutral Coupling of Allenylic Alcohols through Divergent Cooperative Catalysis, *ChemRxiv*, 2025, DOI: **10.26434/chemrxiv-2025-fvz0q**.

6 (*a*) J. Zhang, X. Huo, J. Xiao, L. Zhao, S. Ma and W. Zhang, *J. Am. Chem. Soc.*, 2021, **143**, 12622–12632; (*b*) S. Song, J. Zhou, C. Fu and S. Ma, *Nat. Commun.*, 2019, **10**, 507; (*c*) Q. Li, C. Fu and S. Ma, *Angew. Chem., Int. Ed.*, 2014, **53**, 6511–6514; (*d*) B. Wan and S. Ma, *Angew. Chem., Int. Ed.*, 2013, **52**, 441–445; (*e*) Q. Li, C. Fu and S. Ma, *Angew. Chem., Int. Ed.*, 2012, **51**, 11783–11786; (*f*) B. M. Trost, D. R. Fandrick and D. C. Dinh, *J. Am. Chem. Soc.*, 2005, **127**, 14186–14187.

7 (*a*) M. Isomura, D. A. Petrone and E. M. Carreira, *J. Am. Chem. Soc.*, 2021, **143**, 3323–3329; (*b*) F. Glatz, D. A. Petrone and E. M. Carreira, *Angew. Chem., Int. Ed.*, 2020, **59**, 16404–16408; (*c*) M. Isomura, D. A. Petrone and E. M. Carreira, *J. Am. Chem. Soc.*, 2019, **141**, 4738–4748; (*d*) D. A. Petrone, M. Isomura, I. Franzoni, S. L. Rössler and E. M. Carreira, *J. Am. Chem. Soc.*, 2018, **140**, 4697–4704.

8 (*a*) T. Sawano, M. Kobayashi, M. Ishikawa, E. Ishikawa and R. Takeuchi, *Org. Chem. Front.*, 2025, **12**, 1080–1085; (*b*) S. Mitra and S. Mukherjee, *JACS Au*, 2024, **4**, 4285–4294; (*c*) A. Chakrabarty, K. Jaiswal, M. De and S. Mukherjee, *Org. Chem. Front.*, 2024, **11**, 5107–5115; (*d*) P. Das, D. Ghosh and S. Mukherjee, *Angew. Chem., Int. Ed.*, 2024, **63**, e202413609; (*e*) A. Chakrabarty and S. Mukherjee, *Angew. Chem., Int. Ed.*, 2022, **61**, e202115821.

9 B. M. Trost and J. S. Tracy, *Acc. Chem. Res.*, 2020, **53**, 1568–1579.

10 (*a*) S. Matsubara, T. Okazoe, K. Oshima, K. Takai and H. Nozaki, *Bull. Chem. Soc. Jpn.*, 1985, **58**, 844–849; (*b*) D. Roy, P. Tharra and B. Baire, *Asian J. Org. Chem.c*, 2018, **7**, 1015–1032; (*c*) D. A. Engel and G. B. Dudley, *Org. Biomol. Chem.*, 2009, **7**, 4149–4158.

11 (*a*) B. M. Trost, J. S. Tracy and T. Yusoontorn, *Org. Lett.*, 2019, **21**, 1207–1211; (*b*) B. M. Trost and J. S. Tracy, *Org. Lett.*, 2017, **19**, 2630–2633; (*c*) B. M. Trost and C. Jonasson, *Angew. Chem., Int. Ed.*, 2003, **42**, 2063–2066; (*d*) B. M. Trost, C. Jonasson and M. Wuchrer, *J. Am. Chem. Soc.*, 2001, **123**, 12736–12737.

12 (*a*) R. Zhao, X. Huang, M. Wang, S. Hu, Y. Gao, P. Xu and Y. Zhao, *J. Org. Chem.*, 2020, **85**, 8185–8195; (*b*) V. R. Sabbasani, P. Mamidipalli, H. Lu, Y. Xia and D. Lee, *Org. Lett.*, 2013, **15**, 1552–1555.

13 A. K. Buzas, F. M. Istrate and F. Gagosz, *Org. Lett.*, 2007, **9**, 985–988.

14 (*a*) X. Wang, F. Liu, Z. Yan, Q. Qiang, W. Huang and Z.-Q. Rong, *ACS Catal.*, 2021, **11**, 7319–7326; (*b*) C. Zhu, A. P. Kale, H. Yue and M. Rueping, *JACS Au*, 2021, **1**, 1057–1065; (*c*) R. Jillella, S. Raju, H.-C. Hsiao, D.-S. Hsu and S.-C. Chuang, *Org. Lett.*, 2020, **22**, 6252–6256; (*d*) J. Li, R. Oost, B. Maryasin, L. González and N. Maulide, *Nat. Commun.*, 2019, **10**, 2327; (*e*) A. Lumbroso, N. Abermil and B. Breit, *Chem. Sci.*, 2012, **3**, 789–793.

15 (*a*) J. M. Alonso and P. Almendros, *Adv. Synth. Catal.*, 2023, **365**, 1332–1384; (*b*) J. M. Alonso and P. Almendros, *Chem. Rev.*, 2021, **121**, 4193–4252.

16 B. Alcaide, P. Almendros, S. Cembellín and T. M. del Campo, *Adv. Synth. Catal.*, 2015, **357**, 1070–1078.

17 (*a*) X. Wu, J. Fan, X. Huang and S. Ma, *Org. Chem. Front.*, 2021, **8**, 4432–4437; (*b*) A. S. K. Hashmi, M. C. Blanco, D. Fischer and J. W. Bats, *Eur. J. Org Chem.*, 2006, 1387–1389.

18 (*a*) S. L. Rössler, D. A. Petrone and E. M. Carreira, *Acc. Chem. Res.*, 2019, **52**, 2657–2672; (*b*) C. Defieber, M. A. Ariger, P. Moriel and E. M. Carreira, *Angew. Chem., Int. Ed.*, 2007, **46**, 3139–3143.

19 K. H. Ahn, R. B. Klassen and S. J. Lippard, *Organometallics*, 1990, **9**, 3178–3181.

20 B. H. Lipshutz, J. Keith, P. Papa and R. Vivian, *Tetrahedron Lett.*, 1998, **39**, 4627–4630.

21 E. J. Corey and M. Chaykovsky, *J. Am. Chem. Soc.*, 1962, **84**, 867–868.

22 I. Kadota, L. M. Lutete, A. Shibuya and Y. Yamamoto, *Tetrahedron Lett.*, 2001, **42**, 6207–6210.

23 B. Alcaide, P. Almendros and A. Luna, *Chem. Rev.*, 2009, **109**, 3817–3858.

24 (*a*) C. Estarellas, F. Arioli, M. Pérez, C. Are, D. Hevia, E. Molins, F. J. Luque, J. Bosch and M. Amat, *Eur. J. Org Chem.*, 2017, **2017**, 3969–3979; (*b*) K. Takasu, H. Ohsato, J.-i. Kuroyanagi and M. Ihara, *J. Org. Chem.*, 2002, **67**, 6001–6007.

25 C. Hansch, A. Leo and R. W. Taft, *Chem. Rev.*, 1991, **91**, 165–195.

26 A. E. Reed, R. B. Weinstock and F. Weinhold, *J. Chem. Phys.*, 1985, **83**, 735–746.

27 (*a*) D. Ball, *J. Chem. Educ.*, 1998, **75**, 917; (*b*) Y. C. Almanza-Arjona, J. C. Durán-Álvarez, E. Fernández-Urtusástegui and C. S. Castrejón-Perezyera, *J. Chem. Educ.*, 2022, **99**, 3155–3163.

28 CCDC 2384042: Experimental Crystal Structure Determination, 2024, DOI: **10.5517/ccdc.csd.cc2l0sl0**.